Electronic Supplementary Information

Paracetamol and other Acetanilide analogs as inter-molecular hydrogen bonding assisted diamagnetic CEST MRI Contrast Agents

Subhayan Chakraborty[a], S. Peruncheralathan*[a] and Arindam Ghosh*[a]

[a] School of Chemical Sciences, National Institute of Science Education and Research ,HBNI, At/PO Jatni, Khurdha 752050 ,Odisha,India

Email: peru@niser.ac.in, aringh@niser.ac.in

Table of Content

- **Figures S1-S9:** (a) Overlaid z-spectra for N-phenylacetamide (**1**) with changing saturation power at variable temperature (b) Omega plot for calculation of k_{ex}.

- **Figures S10-S25:** ^{1}H and ^{13}C NMR spectra of compounds **2**-**9** in DMSO-d_6 .

- **Figures S26-S32:** (a) Overlaid z-spectra of compounds **2**-**9** at the physiological condition (b) Overlaid z-spectra of **2-9** with changing saturation power (c) Omega plot for calculation of k_{ex} for compound **2-9**.

- **Figures S33-38:** a) Overlaid z-spectra for N-(4-hydroxyphenyl) acetamide (**9**) with changing saturation power at variable pH ranging from 6.8-8.1 (b) Omega plot for calculation of k_{ex}.

- **Figure S39:** Overlaid z-spectra for N-(4-hydroxyphenyl) acetamide (**9**) with varying pH ranging from 6.8-8.1.

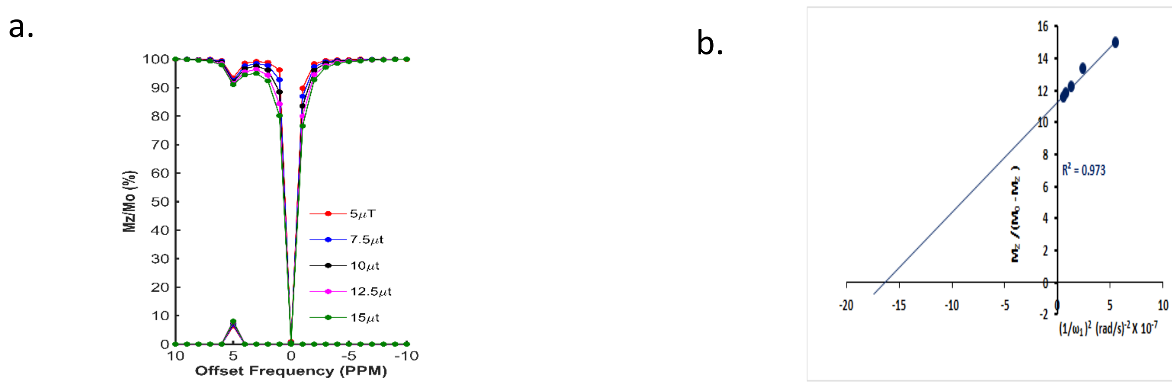

Figure S1: (a) Dependence of CEST percentage on saturation field strength ranging from 5 μT to 15 μT for N-phenylacetamide (**1**) at 298K and pH 7.4 (b) Omega plot for exchange rate measurement. The expected linear relationship of $M_z/(M_0\text{-}M_z)$ as a function of $1/\omega_1^2$ $(\text{rad/sec})^{-2}$ x 10^{-7} was obtained when recorded at 16.3 T of 15 mM compound in 0.01M PBS buffer at pH 7.4. RF saturation pulse was applied for 6 s ensuring complete saturation.

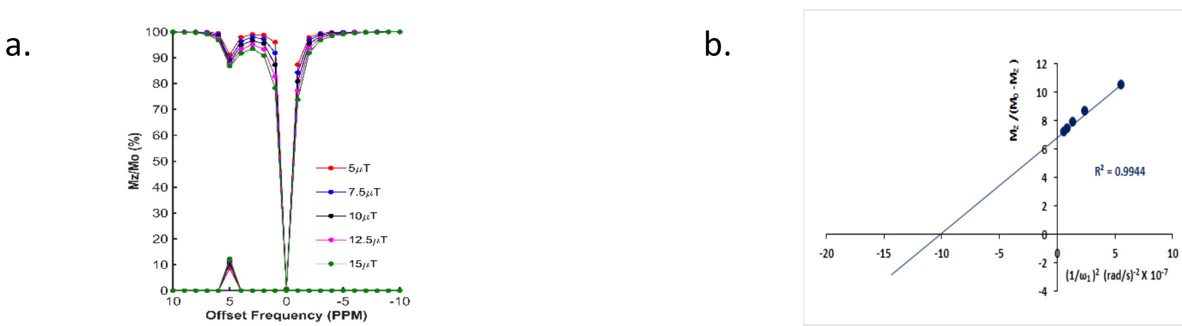

Figure S2: (a) Dependence of CEST percentage on saturation field strength ranging from 5 μT to 15 μT for N-phenylacetamide (**1**) at 303K and pH 7.4 (b) Omega plot for exchange rate measurement. The expected linear relationship of $M_z/(M_0\text{-}M_z)$ as a function of $1/\omega_1^2$ $(\text{rad/sec})^{-2}$ x 10^{-7} was obtained when recorded at 16.3 T of 15 mM compound in 0.01M PBS buffer at pH 7.4. RF saturation pulse was applied for 6 s ensuring complete saturation.

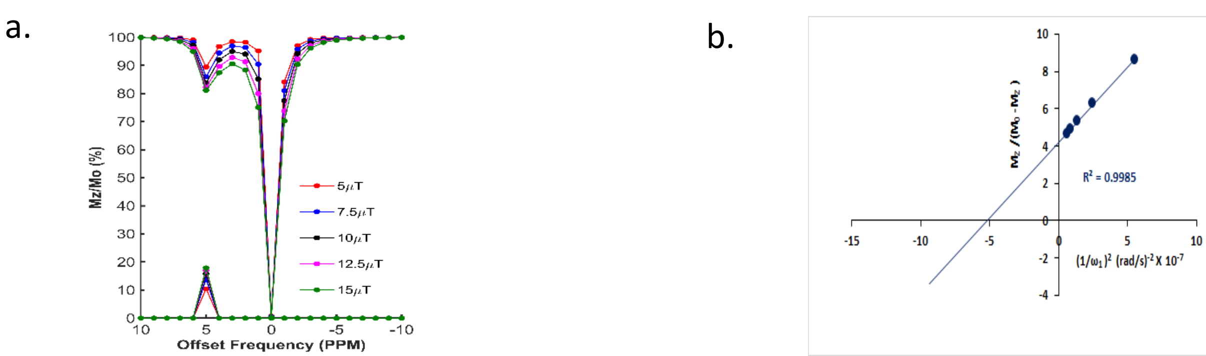

Figure S3: (a) Dependence of CEST percentage on saturation field strength ranging from 5 μT to 15 μT for N-phenylacetamide (**1**) at 308K and pH 7.4 (b) Omega plot for exchange rate measurement. The expected linear relationship of $M_z/(M_0\text{-}M_z)$ as a function of $1/\omega_1^2$ $(\text{rad/sec})^{-2}$ x 10^{-7} was obtained when recorded at 16.3 T of 15 mM compound in 0.01M PBS buffer at pH 7.4. RF saturation pulse was applied for 6 s ensuring complete saturation.

a.

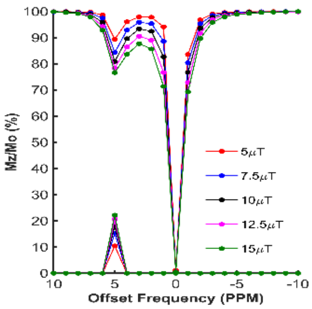

b.

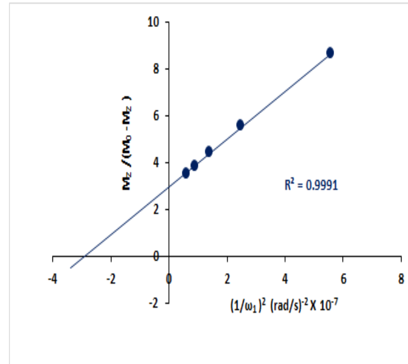

Figure S4: (a) Dependence of CEST percentage on saturation field strength ranging from 5 μT to 15 μT for N-phenylacetamide (**1**) at 310K (b) Omega plot for exchange rate measurement. The expected linear relationship of $M_z/(M_0\text{-}M_z)$ as a function of $1/\omega_1^2$ (rad/sec)$^{-2}$ x 10^{-7} was obtained when recorded at 16.3 T of 15 mM compound in 0.01M PBS buffer at pH 7.4. RF saturation pulse was applied for 6 s ensuring complete saturation.

a.

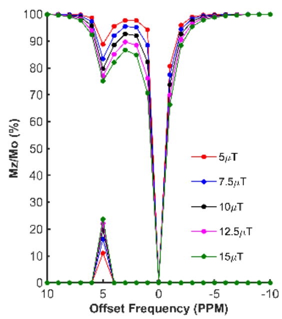

b.

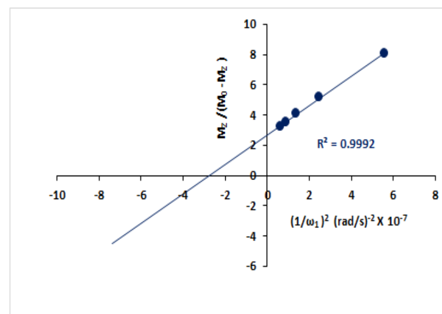

Figure S5: (a) Dependence of CEST percentage on saturation field strength ranging from 5 μT to 15 μT for N-phenylacetamide (**1**) at 313K and pH 7.4 (b) Omega plot for exchange rate measurement. The expected linear relationship of $M_z/(M_0\text{-}M_z)$ as a function of $1/\omega_1^2$ (rad/sec)$^{-2}$ x 10^{-7} was obtained when recorded at 16.3 T of 15 mM compound in 0.01M PBS buffer at pH 7.4. RF saturation pulse was applied for 6 s ensuring complete saturation.

a.

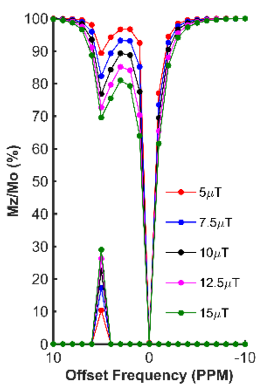

b.

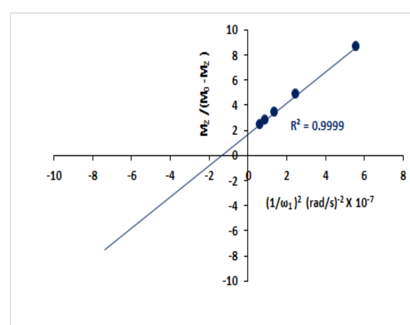

Figure S6: (a) Dependence of CEST percentage on saturation field strength ranging from 5 μT to 15 μT for N-phenylacetamide (**1**) at 318K and pH 7.4 (b) Omega plot for exchange rate measurement. The expected linear relationship of $M_z/(M_0\text{-}M_z)$ as a function of $1/\omega_1^2$ (rad/sec)$^{-2}$ x 10^{-7} was obtained when recorded at 16.3 T of 15 mM compound in 0.01M PBS buffer at pH 7.4. RF saturation pulse was applied for 6 s ensuring complete saturation.

a.

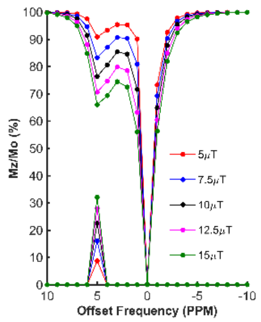

b.

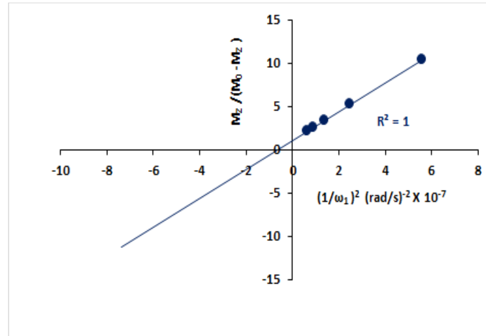

Figure S7: (a) Dependence of CEST percentage on saturation field strength ranging from 5 µT to 15 µT for N-phenylacetamide (**1**) at 323K and pH 7.4 (b) Omega plot for exchange rate measurement. The expected linear relationship of $M_z/(M_0\text{-}M_z)$ as a function of $1/\omega_1^2$ (rad/sec)$^{-2}$ x 10^{-7} was obtained when recorded at 16.3 T of 15 mM compound in 0.01M PBS buffer at pH 7.4. RF saturation pulse was applied for 6 s ensuring complete saturation.

a.

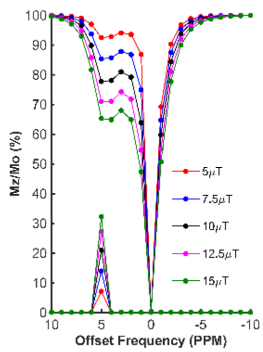

b.

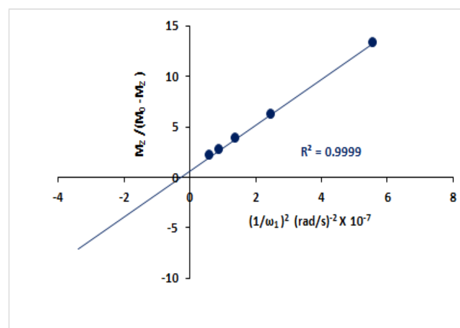

Figure S8: (a) Dependence of CEST percentage on saturation field strength ranging from 5 µT to 15 µT for N-phenylacetamide (**1**) at 328K and pH 7.4 (b) Omega plot for exchange rate measurement. The expected linear relationship of $M_z/(M_0\text{-}M_z)$ as a function of $1/\omega_1^2$ (rad/sec)$^{-2}$ x 10^{-7} was obtained when recorded at 16.3 T of 15 mM compound in 0.01M PBS buffer at pH 7.4. RF saturation pulse was applied for 6 s ensuring complete saturation.

a.

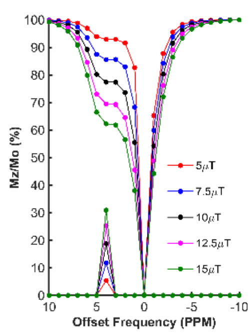

b.

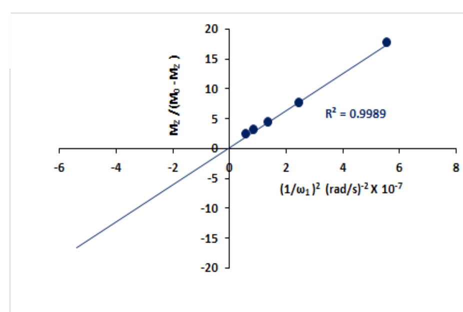

Figure S9: (a) Dependence of CEST percentage on saturation field strength ranging from 5 µT to 15 µT for N-phenylacetamide (**1**) at 333K and pH 7.4 (b) Omega plot for exchange rate measurement. The expected linear relationship of $M_z/(M_0\text{-}M_z)$ as a function of $1/\omega_1^2$ (rad/sec)$^{-2}$ x 10^{-7} was obtained when recorded at 16.3 T of 15 mM compound in 0.01M PBS buffer at pH 7.4. RF saturation pulse was applied for 6 s ensuring complete saturation

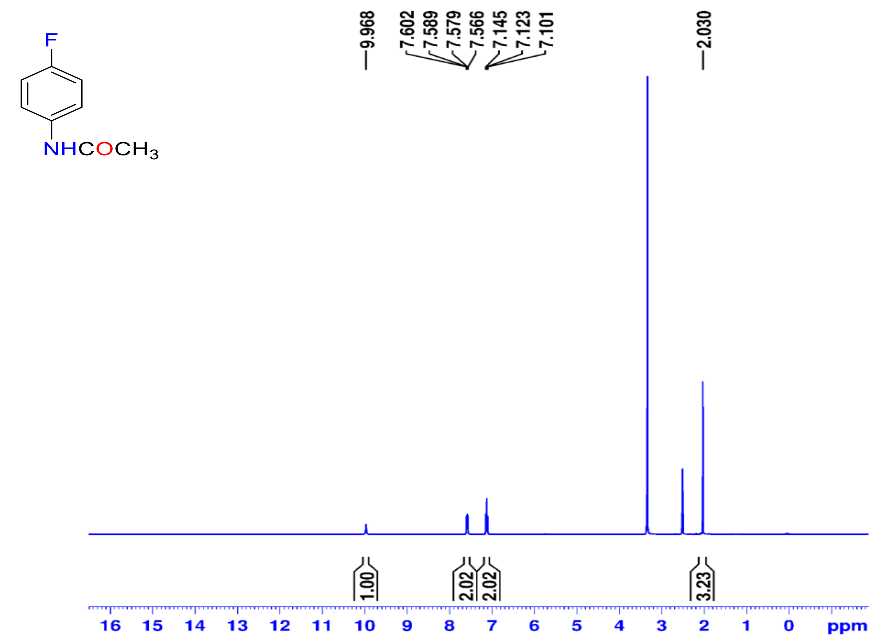

Figure S10: ^{1}H-NMR spectrum of *N*-(4-fluorophenyl)acetamide (**2**) in DMSO-d$_6$ at 298K.

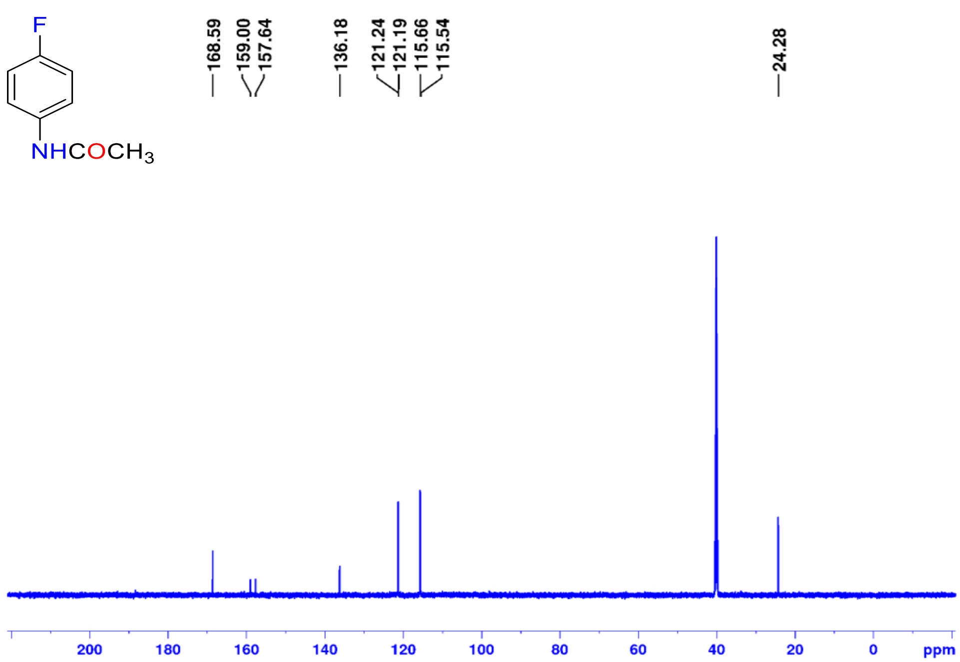

Figure S11: ^{13}C NMR spectrum of *N*-(4-fluorophenyl)acetamide (**2**) in DMSO-d$_6$ at 298K.

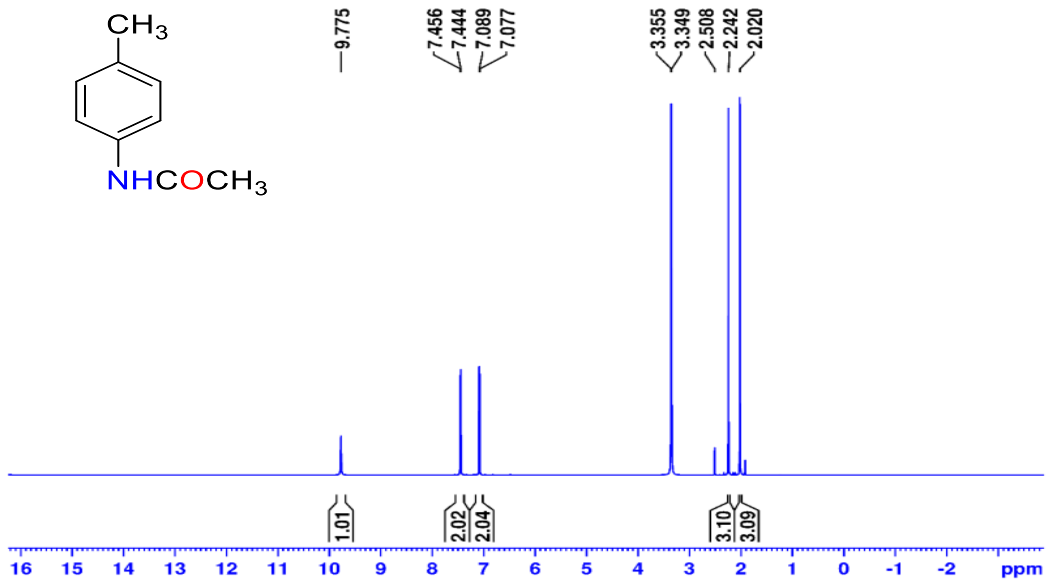

Figure S12: ^{1}H-NMR spectrum of *N*-(p-tolyl)acetamide (**3**) in DMSO-d_6 at 298K.

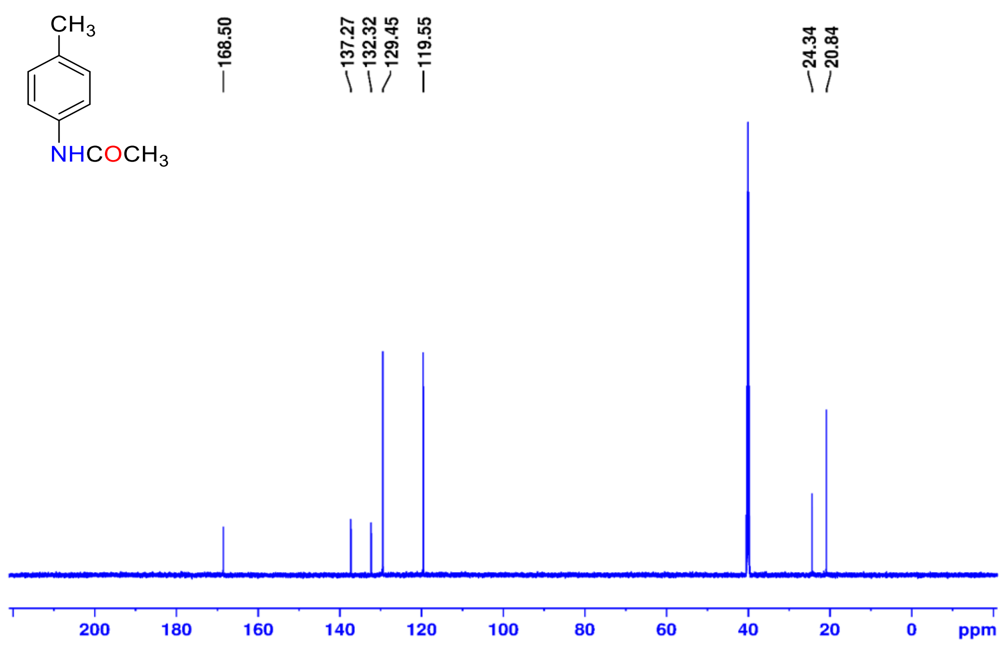

Figure S13: ^{13}C NMR spectrum of *N*-(p-tolyl)acetamide (**3**) in DMSO-d_6 at 298K.

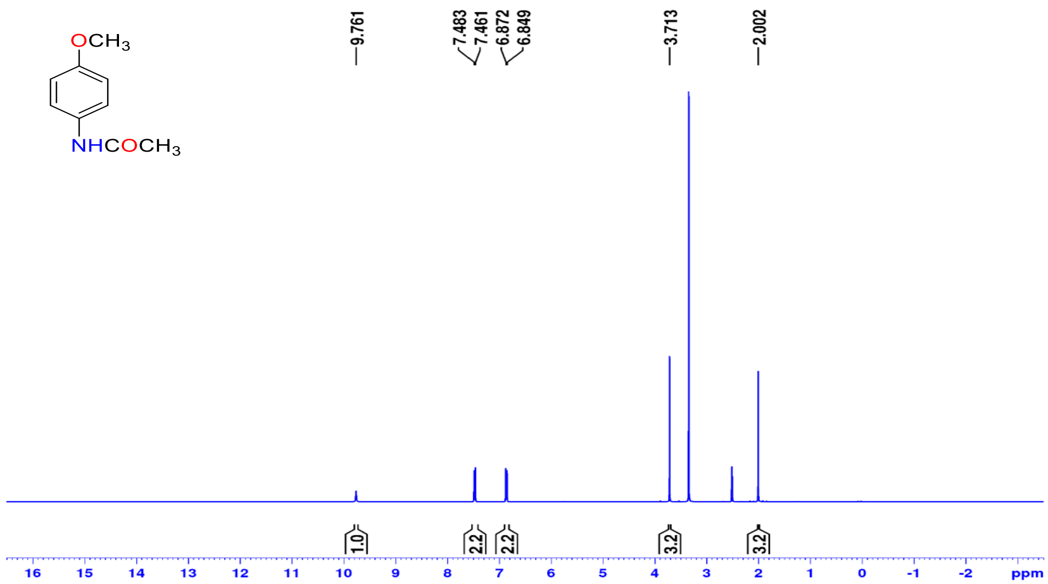

Figure S14: ^{1}H-NMR spectrum of N-(4-methoxyphenyl)acetamide (**4**) in DMSO-d$_6$ at 298K.

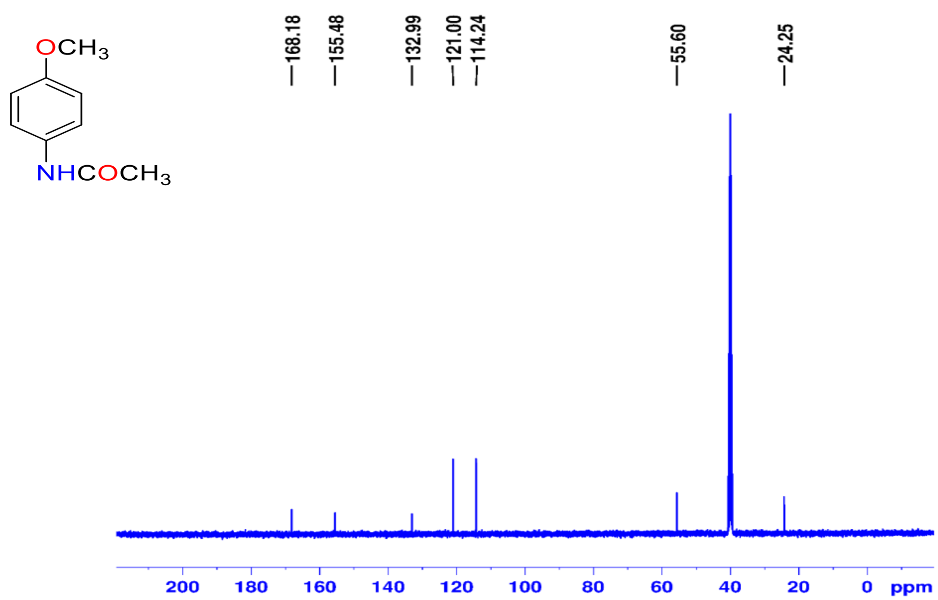

Figure S15: ^{13}C NMR spectrum of N-(4-methoxyphenyl)acetamide (**4**) in DMSO-d$_6$ at 298K.

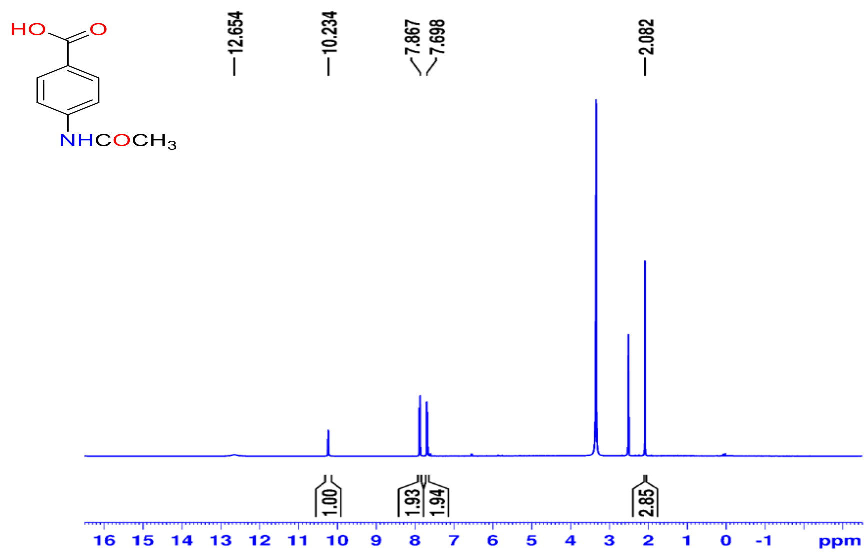

Figure S16: ^{1}H-NMR spectrum of 4-acetamidobenzoic acid **(5)** in DMSO-d$_6$ at 298K.

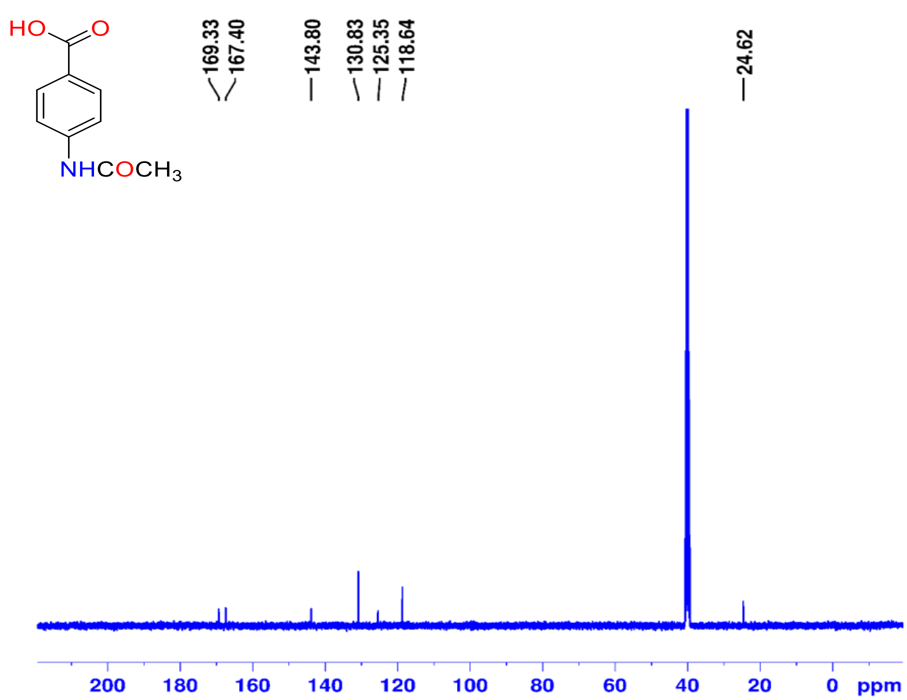

Figure S17: ^{13}C NMR spectrum of 4-acetamidobenzoic acid (**5**) in DMSO-d$_6$ at 298K.

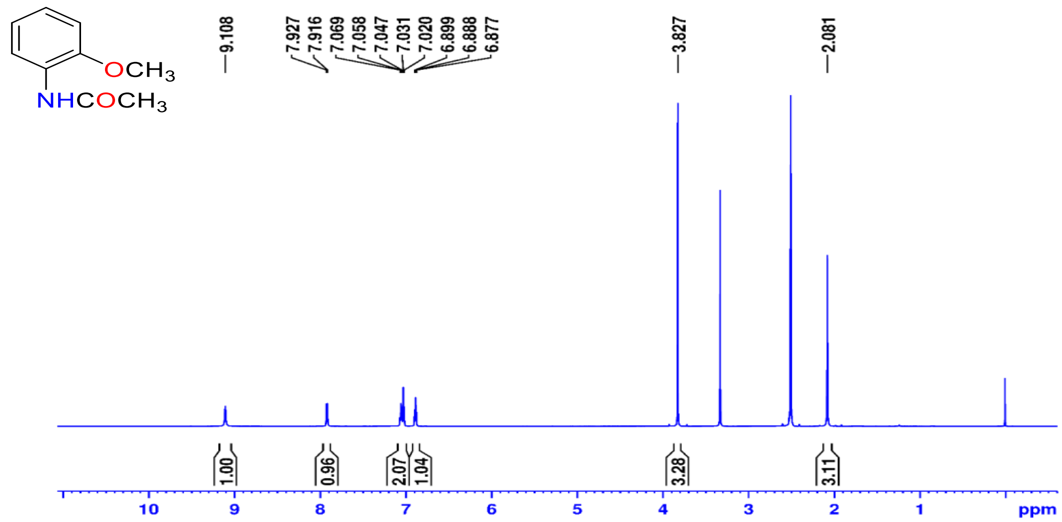

Figure S18: ^{1}H-NMR spectrum of N-(2-methoxyphenyl) acetamide (**6**) in DMSO-d_6 at 298K.

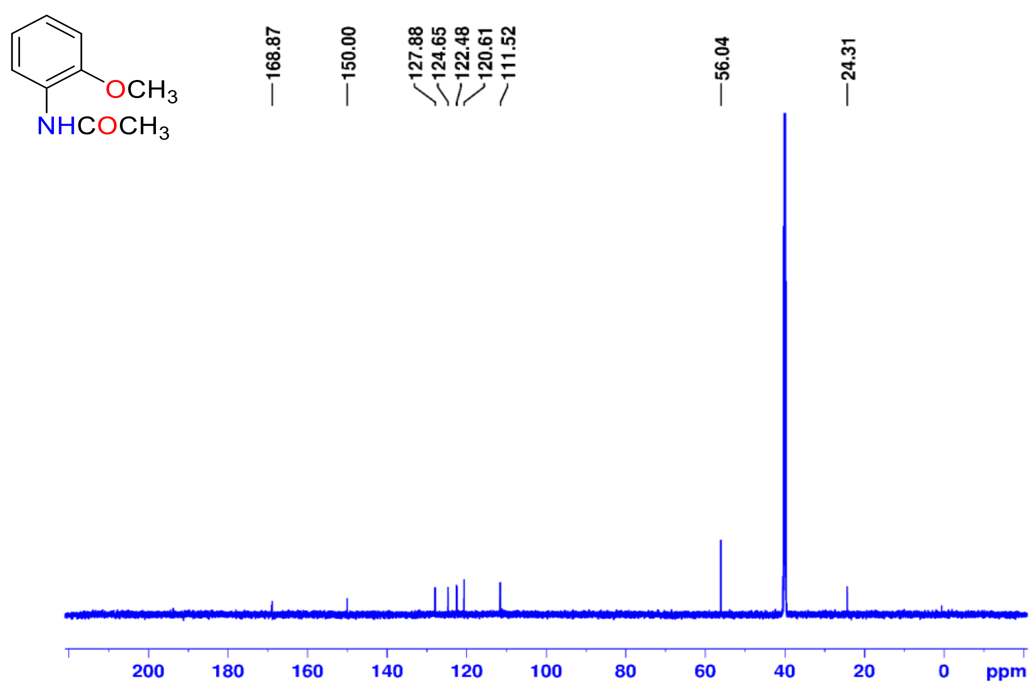

Figure S19: ^{13}C NMR spectrum of N-(2-methoxyphenyl) acetamide (**6**) in DMSO-d_6 at 298K.

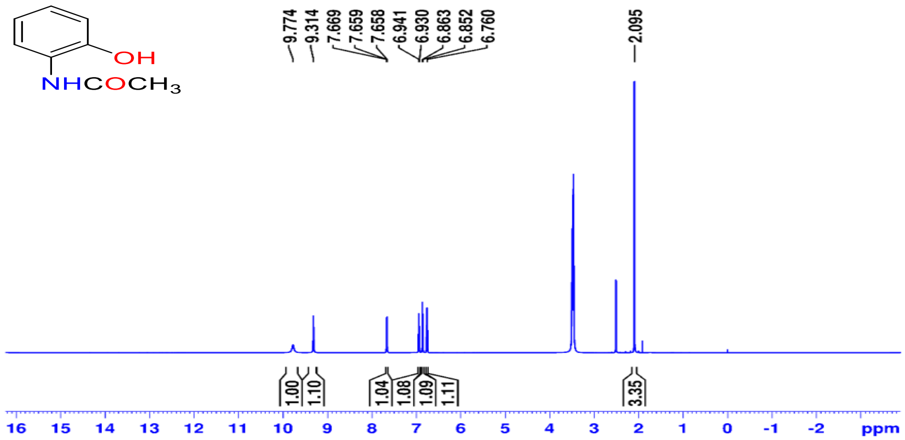

Figure S20: ^{1}H-NMR spectrum of N-(2-hydroxyphenyl)acetamide (**7**) in DMSO-d_6 at 298K.

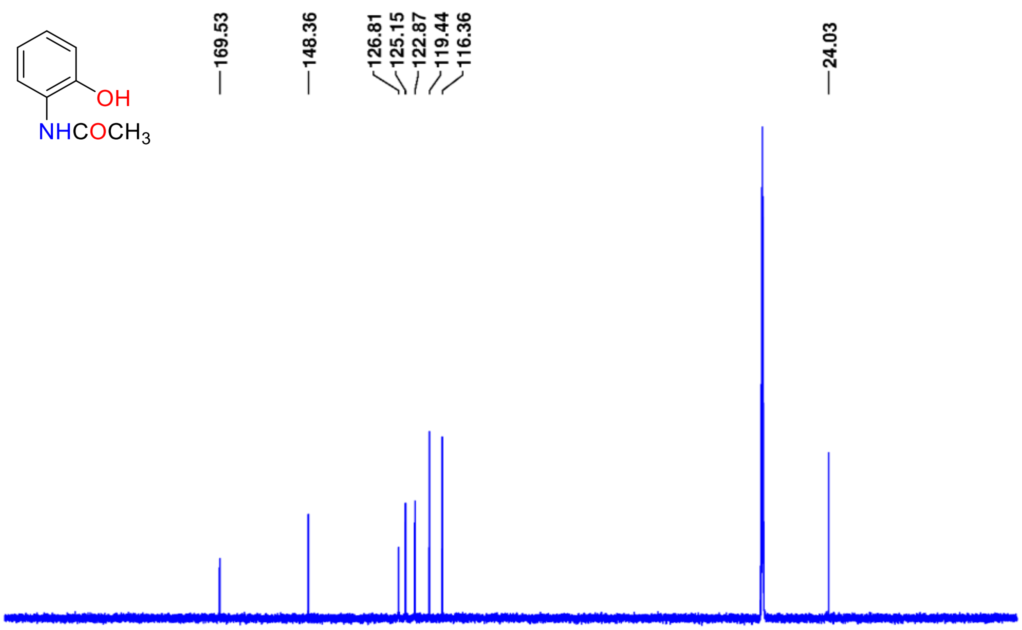

Figure S21: ^{13}C NMR spectrum of N-(2-hydroxyphenyl)acetamide (**7**) in DMSO-d_6 at 298K.

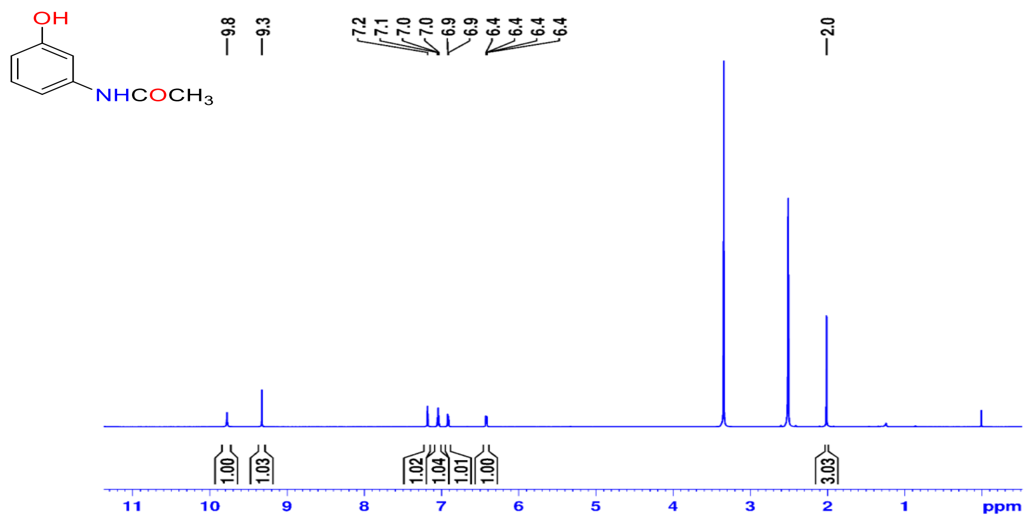

Figure S22: ^{1}H-NMR spectrum of N-(3-hydroxyphenyl) acetamide (**8**) in DMSO-d_6 at 298K.

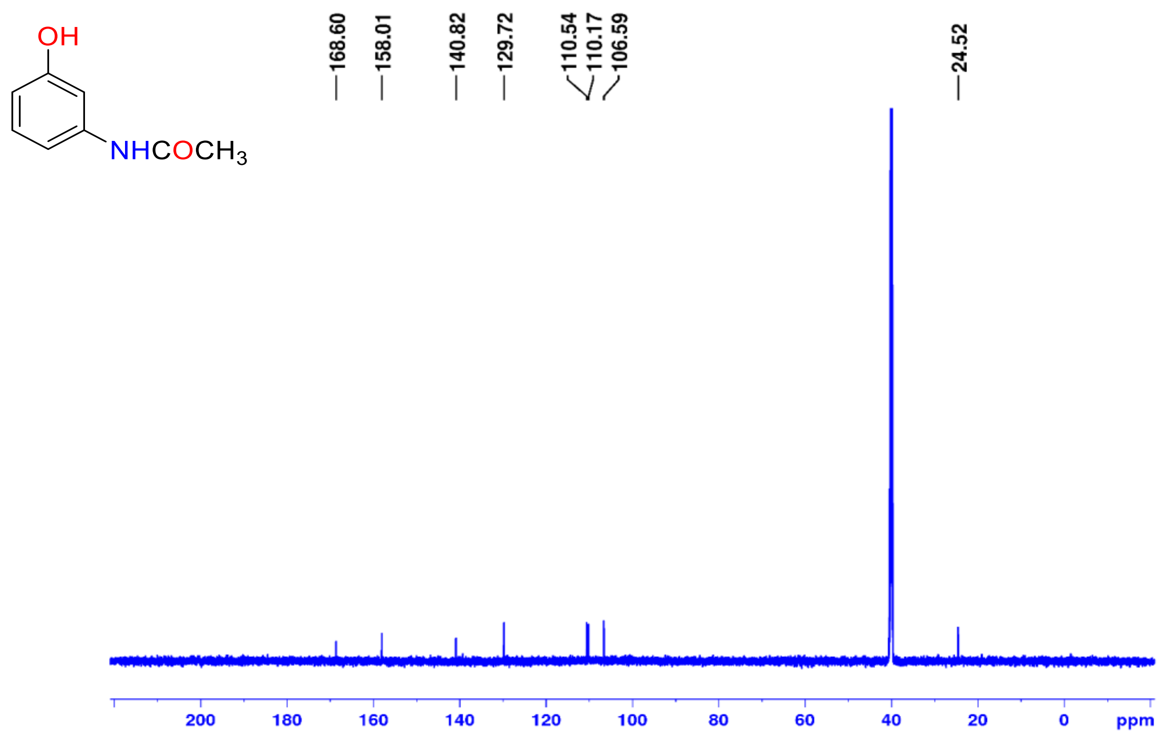

Figure S23: ^{13}C NMR spectrum of N-(3-hydroxyphenyl) acetamide (**8**) in DMSO-d_6 at 298K.

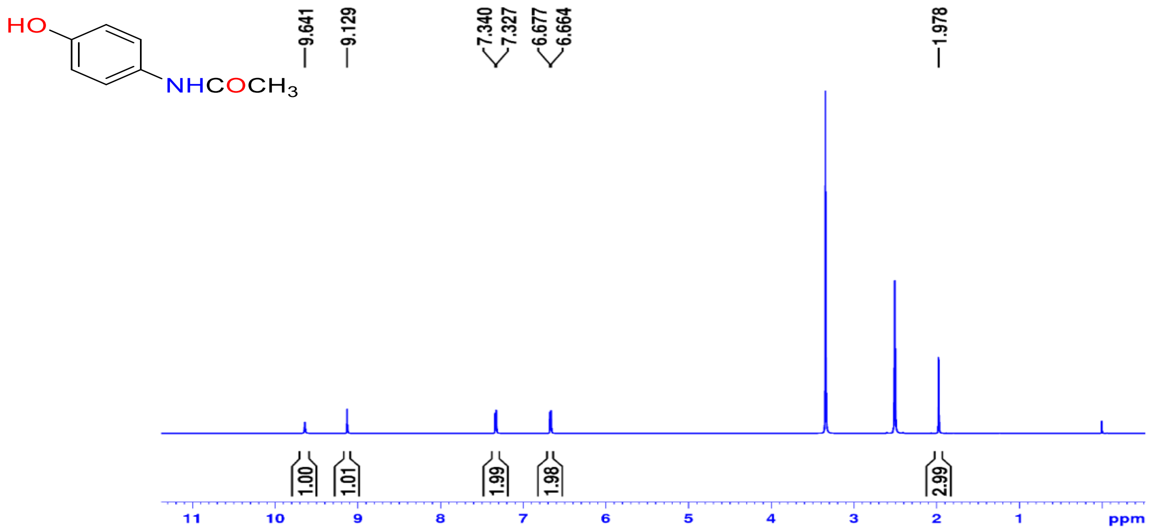

Figure S24: ^{1}H-NMR spectrum of N-(4-hydroxyphenyl) acetamide (**9**) in DMSO-d_6 at 298K.

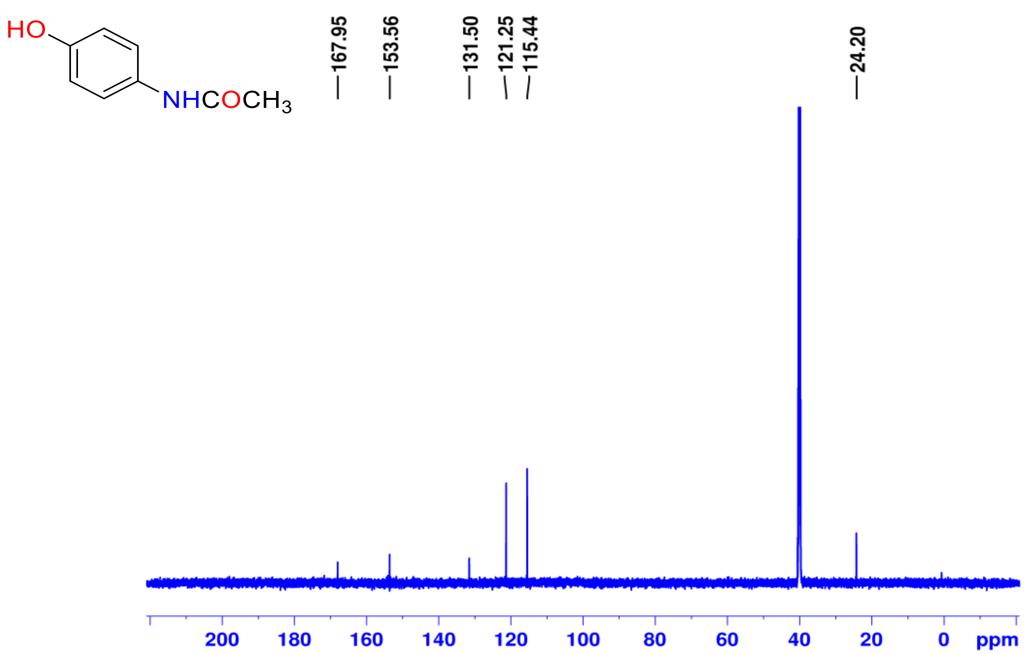

Figure S25: ^{13}C NMR spectrum of N-(4-hydroxyphenyl) acetamide (**9**) in DMSO-d_6 at 298K.

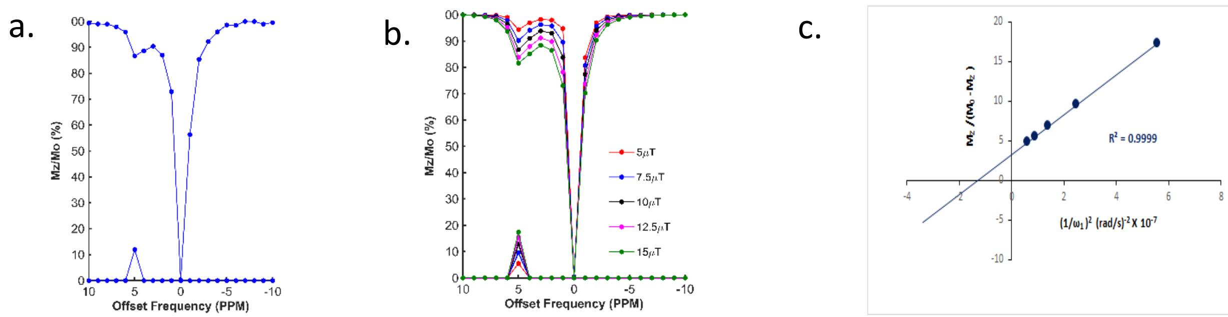

Figure S26: (a) z-spectra of 15mM *N*-(4-fluorophenyl)acetamide (**2**) at 310K and at pH 7.4 recorded at 9.3T (b) Dependence of CEST percentage on saturation field strength ranging from 5μT to 15μT for (2) (c) Omega plot for exchange rate measurement. The expected linear relationship of $M_z/(M_0\text{-}M_z)$ as a function of $1/\omega_1^2$ (rad/sec)$^{-2}$ x 10^{-7} was obtained when recorded at 16.3 T of 15 mM compound in 0.01M PBS buffer at pH 7.4. RF saturation pulse was applied for 6 s ensuring complete saturation.

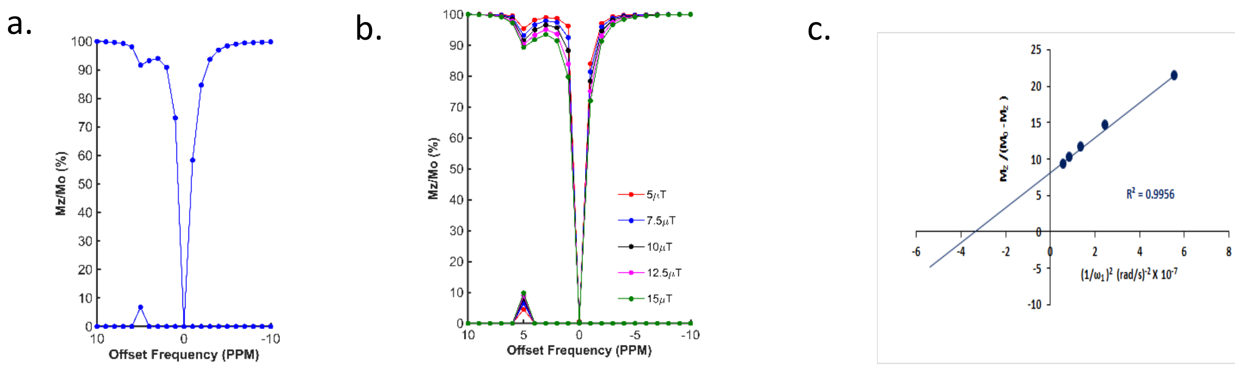

Figure S27: (a) z-spectra of 15mM N-(p-tolyl)acetamide (**3**) at 310K and at pH 7.4 recorded at 9.3T (b) Dependence of CEST percentage on saturation field strength ranging from 5 μT to 15 μT for (3) (c) Omega plot for exchange rate measurement. The expected linear relationship of $M_z/(M_0\text{-}M_z)$ as a function of $1/\omega_1^2$ (rad/sec)$^{-2}$ x 10^{-7} was obtained when recorded at 16.3 T of 15 mM compound in 0.01M PBS buffer at pH 7.4. RF saturation pulse was applied for 6 s ensuring complete saturation.

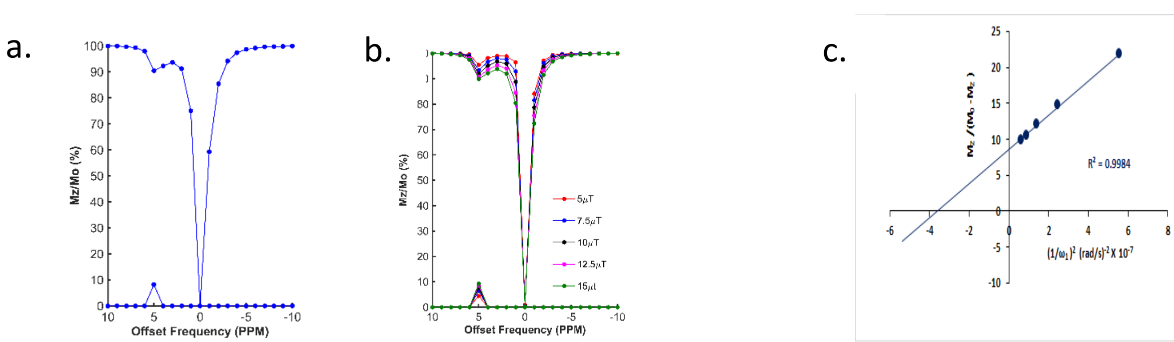

Figure S28: (a) z-spectra of 15mM N-(4-methoxyphenyl)acetamide (**4**) at 310K and at pH 7.4 recorded at 9.3T (b) Dependence of CEST percentage on saturation field strength ranging from 5 μT to 15 μT for (4) (c) Omega plot for exchange rate measurement. The expected linear relationship of $M_z/(M_0\text{-}M_z)$ as a function of $1/\omega_1^2$ (rad/sec)$^{-2}$ x 10^{-7} was obtained when recorded at 16.3 T of 15 mM compound in 0.01M PBS buffer at pH 7.4. RF saturation pulse was applied for 6 s ensuring complete saturation.

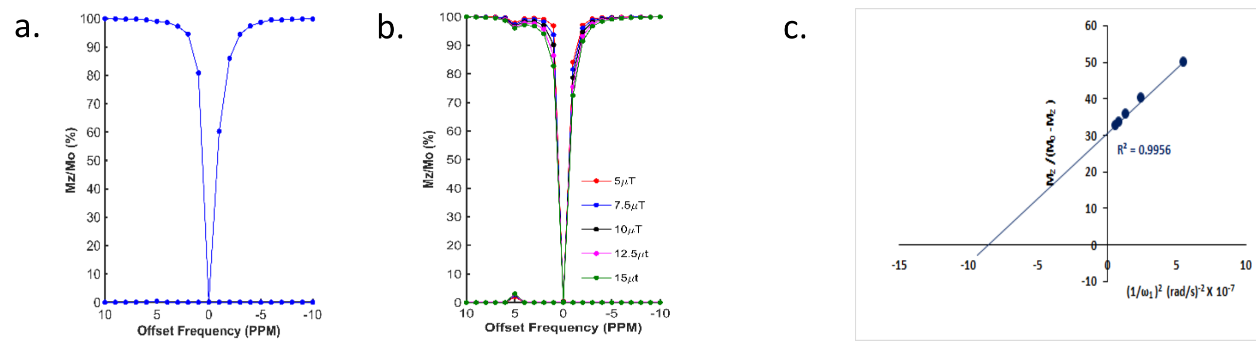

Figure S29: (a) z-spectra of 15mM 4-acetamidobenzoic acid (**5**) at 310K and at pH 7.4 recorded at 9.3T (b) Dependence of CEST percentage on saturation field strength ranging from 5 µT to 15 µT for (5) (c) Omega plot for exchange rate measurement. The expected linear relationship of $M_z/(M_0\text{-}M_z)$ as a function of $1/\omega_1^2$ $(rad/sec)^{-2}$ x 10^{-7} was obtained when recorded at 16.3 T of 15 mM compound in 0.01M PBS buffer at pH 7.4. RF saturation pulse was applied for 6 s ensuring complete saturation.

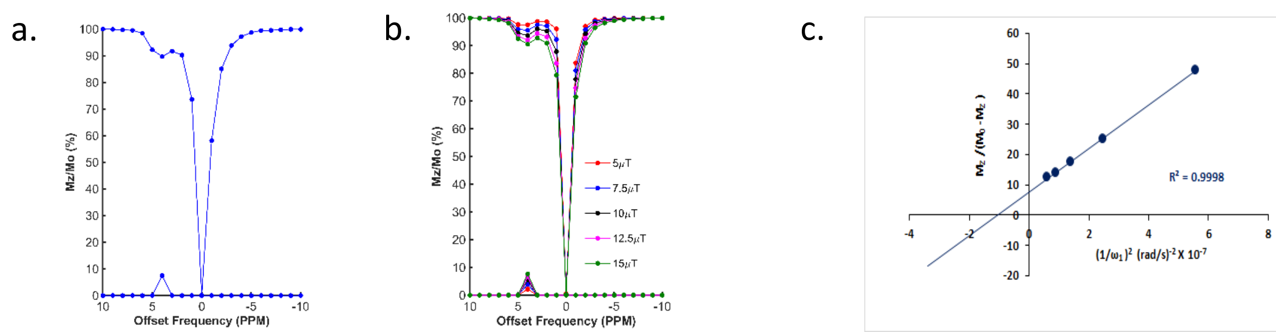

Figure S30: (a) z-spectra of 15mM N-(2-methoxyphenyl)acetamide (**6**) at 310K and at pH 7.4 recorded at 9.3T (b) Dependence of CEST percentage on saturation field strength ranging from 5 µT to 15 µT for (6) (c) Omega plot for exchange rate measurement. The expected linear relationship of $M_z/(M_0\text{-}M_z)$ as a function of $1/\omega_1^2$ $(rad/sec)^{-2}$ x 10^{-7} was obtained when recorded at 16.3 T of 15 mM compound in 0.01M PBS buffer at pH 7.4. RF saturation pulse was applied for 6 s ensuring complete saturation.

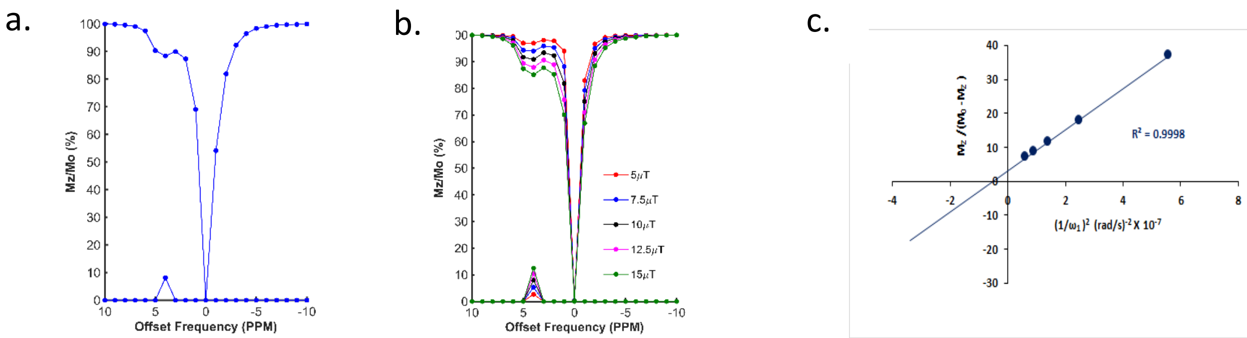

Figure S31: (a) z-spectra of 15mM N-(2-hydroxyphenyl)acetamide (**7**) at 310K and at pH 7.4 recorded at 9.3T (b) Dependence of CEST percentage on saturation field strength ranging from 5 µT to 15 µT for (7) (c) Omega plot for exchange rate measurement. The expected linear relationship of $M_z/(M_0\text{-}M_z)$ as a function of $1/\omega_1^2$ $(rad/sec)^{-2}$ x 10^{-7} was obtained when recorded at 16.3 T of 15 mM compound in 0.01M PBS buffer at pH 7.4. RF saturation pulse was applied for 6 s ensuring complete saturation.

a.

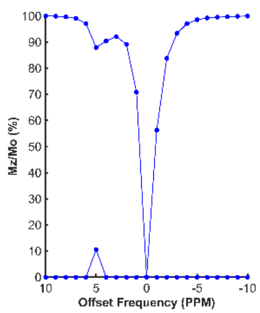

b.

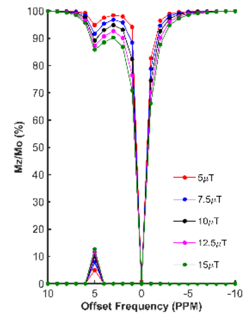

c.

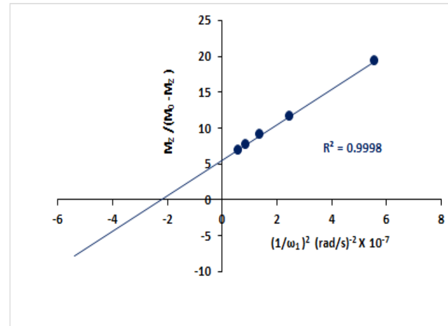

Figure S32: (a) z-spectra of 15mM N-(3-hydroxyphenyl)acetamide (**8**) at 310K and at pH 7.4 recorded at 9.3T (b) Dependence of CEST percentage on saturation field strength ranging from 5 µT to 15 µT for (8) (c) Omega plot for exchange rate measurement. The expected linear relationship of $M_z/(M_0\text{-}M_z)$ as a function of $1/\omega_1^2$ (rad/sec)$^{-2}$ x 10^{-7} was obtained when recorded at 16.3 T of 15 mM compound in 0.01M PBS buffer at pH 7.4. RF saturation pulse was applied for 6 s ensuring complete saturation.

a.

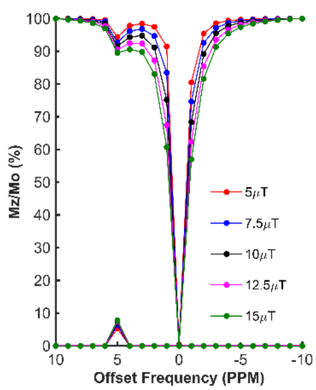

b.

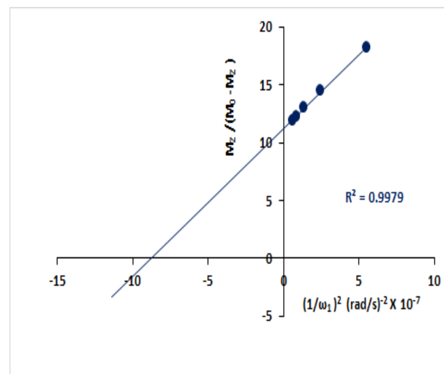

Figure S33: (a) Dependence of CEST percentage on saturation field strength ranging from 5 µT to 15 µT for N-(4-hydroxyphenyl) acetamide (**9**) at pH 6.8. (b) Omega plot for exchange rate measurement. The expected linear relationship of $M_z/(M_0\text{-}M_z)$ as a function of $1/\omega_1^2$ (rad/sec)$^{-2}$ x 10^{-7} was obtained when recorded at 16.3 T of 15 mM compound in 0.01M PBS buffer. RF saturation pulse was applied for 6 s ensuring complete saturation.

a.

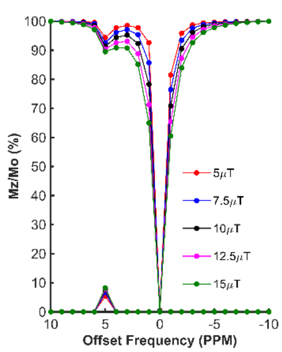

b.

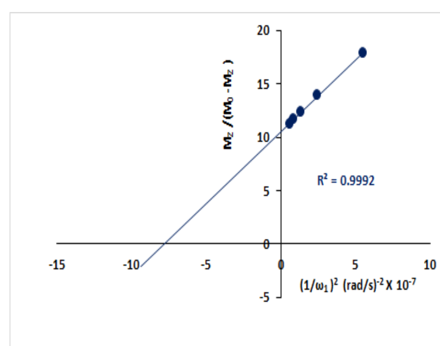

Figure S34: (a) Dependence of CEST percentage on saturation field strength ranging from 5 µT to 15 µT for N-(4-hydroxyphenyl) acetamide (**9**) at pH 7.0. (b) Omega plot for exchange rate measurement. The expected linear relationship of $M_z/(M_0\text{-}M_z)$ as a function of $1/\omega_1^2$ (rad/sec)$^{-2}$ x 10^{-7} was obtained when recorded at 16.3 T of 15 mM compound in 0.01M PBS buffer. RF saturation pulse was applied for 6 s ensuring complete saturation.

a.

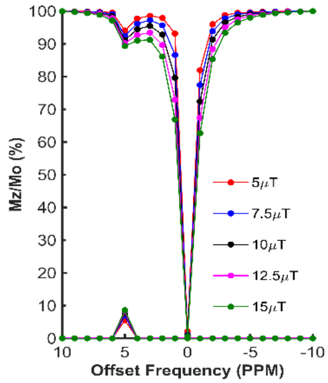

b.

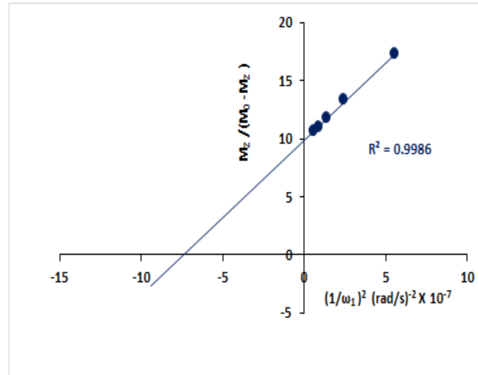

Figure S35: (a) Dependence of CEST percentage on saturation field strength ranging from 5 μT to 15 μT for N-(4-hydroxyphenyl) acetamide (**9**) at pH 7.2 (b) Omega plot for exchange rate measurement. The expected linear relationship of $M_z/(M_0\text{-}M_z)$ as a function of $1/\omega_1^2$ $(\mathrm{rad/sec})^{-2}$ x 10^{-7} was obtained when recorded at 16.3 T of 15 mM compound in 0.01M PBS buffer. RF saturation pulse was applied for 6 s ensuring complete saturation.

a.

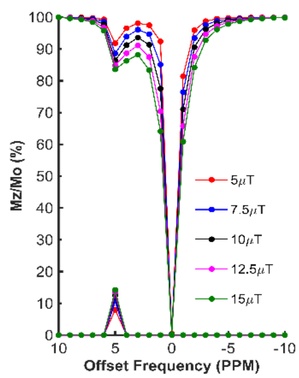

b.

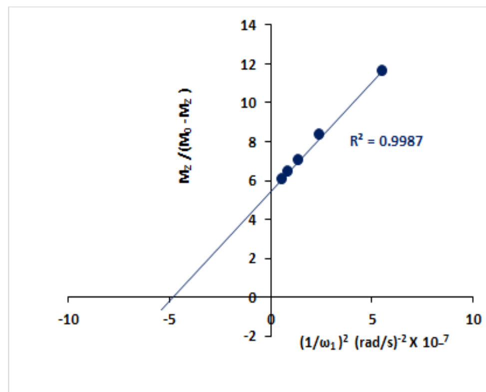

Figure S36: (a) Dependence of CEST percentage on saturation field strength ranging from 5 μT to 15 μT for N-(4-hydroxyphenyl) acetamide (**9**) at pH 7.6 (b) Omega plot for exchange rate measurement. The expected linear relationship of $M_z/(M_0\text{-}M_z)$ as a function of $1/\omega_1^2$ $(\mathrm{rad/sec})^{-2}$ x 10^{-7} was obtained when recorded at 16.3 T of 15 mM compound in 0.01M PBS buffer. RF saturation pulse was applied for 6 s ensuring complete saturation.

a.

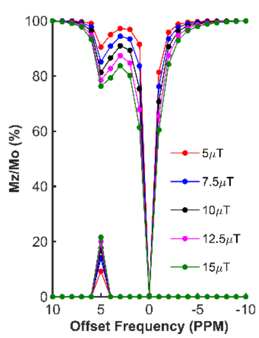

b.

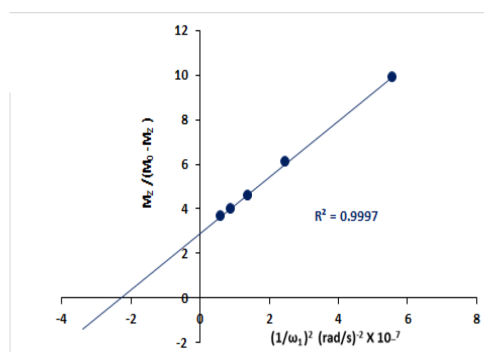

Figure S37: (a) Dependence of CEST percentage on saturation field strength ranging from 5 μT to 15 μT for N-(4-hydroxyphenyl) acetamide (**9**) at pH 7.9 (b) Omega plot for exchange rate measurement. The expected linear relationship of $M_z/(M_0\text{-}M_z)$ as a function of $1/\omega_1^2$ $(\mathrm{rad/sec})^{-2}$ x 10^{-7} was obtained when recorded at 16.3 T of 15 mM compound in 0.01M PBS buffer. RF saturation pulse was applied for 6 s ensuring complete saturation.

a.

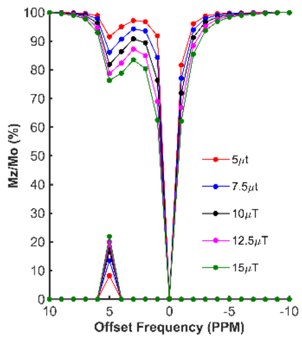

b.

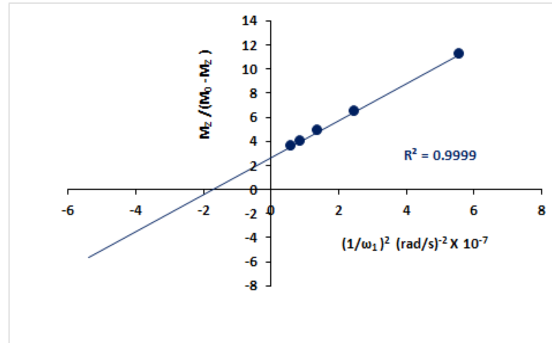

Figure S38: (a) Dependence of CEST percentage on saturation field strength ranging from 5 µT to 15 µT for N-(4-hydroxyphenyl) acetamide (**9**) at pH 8.1 .(b) Omega plot for exchange rate measurement. The expected linear relationship of $M_z/(M_0-M_z)$ as a function of $1/\omega_1^2$ $(rad/sec)^{-2} \times 10^{-7}$ was obtained when recorded at 16.3 T of 15 mM compound in 0.01M PBS buffer. RF saturation pulse was applied for 6 s ensuring complete saturation.

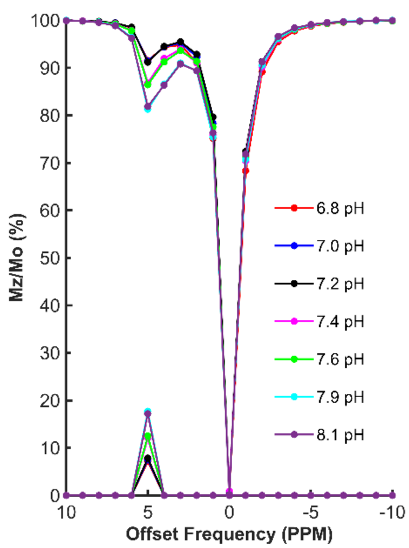

Figure S39: Dependence of CEST effect of N-(4-hydroxyphenyl) acetamide (**9**) on pH. Overlaid Z-spectra with pH ranging from 6.8 to 8.1. 5 µT RF saturation was applied for 3s to obtain the z-spectra.